Journal of Cellular Biochemistry 67:514–527 (1997)

Actin Isoform Utilization During Differentiation and Remodeling of BC3H1 Myogenic Cells

Guang Qu, Hua Yan, and Arthur R. Strauch*

Department of Cell Biology, Neurobiology, and Anatomy, The Ohio State University, College of Medicine, Columbus, Ohio 43210-1239

Abstract Mouse BC3H1 myogenic cells and a bi-functional chemical cross linking reagent were utilized to investigate the polymerization of newly-synthesized vascular smooth muscle (α-actin) and non-muscle (β- and γ-actin) actin monomers into native F-actin filament structures during myogenesis. Two actin dimer species were identified by SDS-PAGE analysis of phenylenebismaleimide-cross linked fractions of BC3H1 myoblasts and myocytes. P-dimer was derived from the F-actin-enriched, detergent-insoluble cytoskeleton. Pulse-chase analysis revealed that D-dimer initially was associated with the cytoskeleton but then accumulated in the soluble fraction of lysed muscle cells that contained a non-filamentous or aggregated actin pool. Immunoblot analysis indicated that non-muscle and smooth muscle actins were capable of forming both types of dimer. However, induction of smooth muscle α-actin in developing myoblasts coincided with an increase in D-dimer level which may facilitate actin stress fiber assembly. Smooth muscle α-actin was rapidly utilized in differentiating myoblasts to assemble extraction-resistant F-actin filaments in the cytoskeleton whereas non-muscle β- and γ-actin filaments were more readily dissociated from the cytoskeleton by an extraction buffer containing ATP and EGTA. The data indicate that cytoarchitectural remodeling in developing BC3H1 myogenic cells is accompanied by selective actin isoform utilization that effectively segregates multiple isoactins into different sub-cellular domains and/or supramolecular entities. J. Cell. Biochem. 67:514–527, 1997. © 1997 Wiley-Liss, Inc.

Key words: smooth muscle; actin; myogenesis; cytoskeleton; microfilaments; protein crosslinking; muscle cells; cell fractionation

The muscle protein actin performs an essential role in cell motility, muscle contraction, and in the maintainance of cellular shape. At least six actin isoforms exist in vertebrates that are encoded by unique genes [Vandekerckhove and Weber, 1981] and expressed in distinct developmental and tissue-specific patterns [Kedes and Stockdale, 1989; McHugh et al., 1991]. Although the functional significance of multiple actins is not known, the developmentally timed expression of different actin genes may reflect cellular physiological requirements for specialized actin molecules [Korn, 1978; Pardo et al., 1983; Herman, 1993]. For example, actin isoform switching occurs early during myogenesis and cardiogenesis and involves nearly complete replacement of generic β- and γ-actins in immature myoblasts with skeletal or cardiac muscle-specific α-actin isoforms. While expression of these striated muscle α-actins is highly tissue restricted, the vascular smooth muscle α-actin (VSM α-actin) gene is more permissively expressed in a variety of cell lineages and often is co-expressed in varying amounts with non-muscle actins. VSM α-actin not only is the primary actin isoform in adult vascular smooth muscle tissue but also is induced during early cardiac [Ruzicka and Schwartz, 1988] and skeletal muscle development [Sawtell and Lessard, 1989], in myofibroblast-like cell types associated with wound healing [Sappino et al., 1990; Skalli and Gabbiani, 1988; Darby et al., 1990], and following cardiac muscle remodeling in response to hemodynamic pressure overload [Black et al., 1991; Parker and Schneider, 1991].

Morphological studies have indicated differences in the sub-cellular distribution of individual actin isoforms [Herman, 1993]. In avian gizzard smooth muscle cells, enteric smooth muscle γ-actin was found to co-localize with

Contract grant sponsor: National Heart, Lung, Blood Institute; Contract grant number: HL-38694.

*Correspondence to: Arthur R. Strauch, Ph.D., Department of Cell Biology, Neurobiology and Anatomy, The Ohio State University, College of Medicine, 333 West 10th Avenue, Columbus, OH 43210-1239.

Received 16 April 1997; Accepted 13 August 1997

© 1997 Wiley-Liss, Inc.

myosin filaments whereas non-muscle β- and γ-actins were more likely to associate with dense bodies, in channels linking adjacent dense bodies, and in membrane-associated dense plaques [North et al., 1994]. Isoform-specific antibodies were utilized by DeNofrio et al. [1989] to identify non-muscle β- and γ-actin enriched compartments in the ruffling, peripheral regions of motile microvascular pericytes. In contrast, smooth muscle α-actin appeared to be confined to centrally located stress fibers within these cells. Interestingly, the localization of VSM α-actin in static actin bundles within pericytes was different from the distribution of evolutionarily related enteric smooth muscle γ-actin, which appeared to co-localize with myosin filaments in chicken gizzard smooth muscle cells [North et al., 1994]. Although individual members of the actin isoform family share very similar amino acid sequences, experimental manipulation of actin isoform stoichiometry in living cells suggests that each type of actin may in fact encode distinct cytoarchitectural information. Expression of cloned β-actin and γ-actin cDNAs in transfected myoblasts revealed that the two actin polypeptides had different effects on cell morphology. β-actin transfectants displayed well-defined filaments whereas γ-actin transfectants exhibited more diffuse arrays of short actin cables [Schevzov et al., 1992]. Other investigators used epitope tagged actin isoforms to demonstrate preferential localization of non-muscle β- and γ-actins at sub-membranous sites in neonatal rat cardiomyocytes [von Arx et al., 1995]. In addition, formation of filopodia and dissolution of pre-existing sarcomeres were observed in cardiomyocytes that over-expressed generic non-muscle actins but not in control cells transfected with muscle α-actin expression plasmids. Cardiomyocytes that contained excess tagged non-muscle γ-actin also were impaired in their ability to spontaneously contract in culture. Tagged VSM α-actin frequently was localized to stress fiber-like structures in cardiomyocytes compared to ectopic striated α-actins that were completely restricted to sarcomeres [von Arx et al., 1995; Perriard et al., 1992]. Interestingly, in human myofibroblasts, the induction of VSM α-actin expression was accompanied by significant impairment of cell motility [Ronnov-Jessen and Petersen, 1996]. Electroporation of a VSM α-actin antibody or anti-sense oligodeoxynucleotides specific for certain segments of the VSM α-actin transcript stimulated migratory behavior presumably by interfering with either smooth muscle α-actin biosynthesis or assembly into stress fibers. The investigators suggested that an important function of VSM α-actin is to immobilize myofibroblasts and enhance cell-substratum traction by laying down rigid stress fibers that would facilitate the wound healing process [Ronnov-Jessen and Petersen, 1996].

The issue of whether newly synthesized VSM α-actin monomers are predisposed to form F-actin filament bundles in cells has not been examined biochemically. Of particular interest is the potential contribution of selective isoform sorting in governing cytoarchitectural remodeling in cell types such as myoblasts, which undergo extensive changes in form and function during development. Vascular smooth muscle cells isolated from aorta potentially are useful for biochemical analysis of actin isoform utilization because non-muscle and smooth muscle actin isoforms are co-expressed in approximately equal amounts in these highly elongated, contractile cells. However, the primary obstacle in using cultured smooth muscle as a model system has been their tendency to irreversibly modulate following exposure to serum mitogens in vitro [Kocher and Gabbiani, 1987; Schwartz and Reidy, 1987]. Cultured smooth muscle cells resemble abnormal smooth muscle cells in vascular lesions with regard to their fibroblastoid appearance and diminished expression of smooth muscle phenotypic marker proteins including VSM α-actin. The mouse BC3H1 myogenic cell line has been employed in our laboratory as an alternative model cell system to investigate the biochemical aspects of actin compartmentalization since smooth muscle actin isoform expression and cytoarchitectural remodeling in these cells can be controlled experimentally by manipulating culture conditions [Schubert et al., 1974; Strauch and Rubenstein, 1984a]. BC3H1 myoblast differentiation is stimulated by high cell density and serum-free medium, fully reversible, and coincides with cellular elongation and a coordinate increase in VSM α-actin expression and decrease in non-muscle β- and γ-actin expression [Strauch and Rubenstein, 1984a; Strauch et al., 1991]. In this report we utilized BC3H1 cells to investigate how newly synthesized VSM α-actin monomers become associated with native actin filamentous structures in situ and whether non-muscle and smooth muscle actin isoforms

are selectively or randomly utilized to assemble cytoarchitectural elements. Our data suggest that mechanisms exist in muscle cells that govern the targeting of actin polypeptides to distinct sub-cellular actin domains.

METHODS

Cell Culture Methods

Stock cultures of mouse BC3H1 myogenic cells were obtained from Dr. David Schubert at the Salk Institute, La Jolla, CA, and maintained in logarithmic stage growth [Schubert et al., 1974; Strauch and Rubenstein, 1984a] by cultivation in Dulbecco's Modified Eagle's Medium (DMEM) supplemented with 1g/L glucose, 10% heat-inactivated fetal bovine serum [Gibco/BRL, Grand Island, NY], 0.32 mg/ml L-glutamine, 100 µg/ml penicillin, and 100 µg/ml streptomycin (Gibco/BRL). Myoblasts were collected for analysis at several culture densities: sub-confluent myoblasts (30–40% confluent, sub-mb), pre-confluent myoblasts (70–80% confluent, pre-mb), and post-confluent myoblasts (100% confluent, post-mb). To induce cytodifferentiation, post-confluent myoblasts were treated for varying periods with serum-free N2 medium [Bottenstein and Sato, 1979; Strauch and Rubenstein, 1984a] containing RPMI 1640, 5 µM bovine serum albumin, 5 µg/ml insulin, 100 µg/ml transferrin, 20 nM progesterone, 100 µM putrescine, 30 nM sodium selenite, 10 nM 4-(2-hydroxyethyl)-l-piperazineethane sulfonic acid (HEPES, Sigma Chemical Co., St. Louis, MO), 100 U/ml penicillin, 100 µg/ml streptomycin, and 0.25 µg/ml Fungizone™ (Gibco/BRL), pH 7.2. Cultures were re-fed with the appropriate medium every third day. For some experiments, cells were radiolabeled at 37°C for 8–12 h with 50 µCi/ml of L-[^{35}S]cysteine or L-[^{35}S]methionine (1,200 Ci/mmol, ICN Biochemicals, Costa Mesa, CA) using either cysteine- or methionine-free N2 labeling medium for differentiated myocytes, or methionine-free DMEM labeling medium for myoblasts. For pulse/chase isotope incorporation studies, cells at different stages of differentiation (indicated in the figure legends) were exposed to the appropriate labeling medium containing 50 µCi/ml L[^{35}S]methionine for 10 min. After 4 washes with Dulbecco's phosphate buffered saline (PBS), the cells were incubated for the indicated periods at 37°C with chase medium containing 5-fold mole excess amounts of unlabeled methionine and cysteine in the appropriate medium formulation.

Actin Polypeptide Purification and Chemical Crosslinking

Purified rabbit skeletal muscle [Spudich and Watt, 1971] or porcine brain [Uyemura et al., 1978] G-actin (1 mg/ml) was polymerized in a buffer containing 5 mM Tris-HCl, pH 8.3, 0.5 mM ATP, 0.2 mM $CaCl_2$, 0.1 M NaCl, and 2 mM $MgCl_2$ at room temperature for 30 min. The resulting F-actin filaments were crosslinked at 22°C using N,N′-1,4-phenylenebismaleimide (PBM, 3 mg/ml in 100% dimethylformamide, Aldrich Chemical Co., Milwaukee, WI) using a molar ratio of 0.5:1.0 (PBM:actin). The crosslinking reaction was quenched by adding 150-fold mole excess of β-mercaptoethanol and the resulting crosslinked actin was analyzed by SDS-PAGE using 10% acrylamide gels. Additionally, actin oligomers generated from sonicated F-actin or F-actin bundles (magnesium paracrystals) prepared by polymerizing G-actin for 30 min in buffer containing 5 mM Tris-HCl, pH 8.3, 0.5 mM ATP, 0.2 mM $CaCl_2$, 0.1 M NaCl, 50 mM $MgCl_2$ were subjected to PBM crosslinking and SDS-PAGE as described above.

Cell Fractionation and In Situ Chemical Crosslinking of Actin Assemblies in BC3H1 Myogenic Cells

Sub-confluent myoblasts, pre-confluent myoblasts, post-confluent myoblasts, and fully differentiated myocytes were incubated for 10 min at room temperature with substrate adhesion buffer containing 50 mM 2-[-morpholino]ethensulfonic acid (MES, Sigma), pH 6 and 5 mM $CaCl_2$ to stabilize cell-substratum adhesion and then lysed at 2°C by a 5-min treatment with lysis buffer containing 10 mM HEPES, pH 6.8, 0.1 M NaCl, 3 mM $MgCl_2$, 0.3 M ultra pure sucrose, 1 mM phenylmethyl sulfonyl fluoride (PMSF), and 0.5% Triton X-100. The released protein solution was collected (referred to as soluble fraction) and adjusted to pH 8.3 using 5M Tris base. Protein residue remaining on the culture dish after lysis (referred to as cytoskeleton fraction) was washed once with lysis buffer and then exposed to crosslinking buffer containing 5 mM Tris-HCl, pH 8.3, 0.5 mM ATP, 0.2 mM $CaCl_2$, 0.1 M NaCl, and 2 mM $MgCl_2$. The soluble and cytoskeleton fractions were combined with PBM for 15 min at 22°C (0.5:1.0,

PBM:actin) and the resulting crosslinked actins were isolated by DNase-I affinity chromatography after first quenching the crosslinking reaction with a 150-fold mole excess of β-mercaptoethanol.

DNase-1 Affinity Chromatography, SDS-PAGE, Immunoblotting, and Isoelectric Focusing Gel Electrophoresis

Crosslinked actin species were isolated using DNase-I affinity chromatography [Lazarides and Lindberg, 1974; Strauch and Rubenstein, 1984a]. Both the soluble and cytoskeleton fractions were combined with an equal volume of 2 × actin depolymerization buffer (1 × buffer contains 0.75 M guanidine hydrochloride, 0.5 M sodium acetate, 10 mM Tris-HCl, pH 7.5, 0.5 mM $CaCl_2$, 0.5 mM ATP, 0.5% Triton X-100, and 1 mM PMSF) and further extracted for 1 to 2 h on ice. After 90 s of sonication, the ice-cold protein solutions were centrifuged for 3 h at 100,000*g* at 4°C to remove insoluble debris. The supernatants were applied to DNase-I-agarose affinity columns (1 ml bed volume), which was washed with 10 bed volumes of actin depolymerization buffer and eluted with 10 bed volumes of a buffer containing 3 M guanidine hydrochloride, 0.5 M sodium acetate, and 2 mM $CaCl_2$. Actin samples were dialyzed repeatedly against large volumes of distilled water at 4°C, lyophilized to dryness, and analyzed by SDS-PAGE (10% gels) and autoradiography (XAR-5 film, Eastman Kodak, Rochester, NY). For immunoblot analysis of crosslinked actins, SDS gels were equilibrated after electrophoresis with transfer buffer containing 25 mM Tris-HCl, 20 mM glycine, and 20% methanol, pH 8.3, and then electrophoretically transferred to nitrocellulose membranes (Duralose, Schleicher & Schuell, Keene, NH) using constant current (300 mA) for 5 h at room temperature. Transfer blots were reacted with either a pan-specific actin monoclonal antibody C4 (provided by James L. Lessard, Children's Hospital Research Foundation, Cincinnati, OH, used at 1:600 dilution) or monoclonal antibody 1A4 (specific for VSM α-actin, used at 1:600 dilution, Sigma) in Tris-buffered saline (TBS) containing 3% BSA. Actin blots were washed three times with TBS and then reacted with peroxidase-labelled goat anti-mouse IgG (Hyclone, Logan, UT, 1:600) at room temperature for 1.5 h. Bound antibody was detected on washed blots by incubating in TBS containing 1.6 mM 4-chloro-1-naphthol and 0.2% (v/v) hydrogen peroxide. Isoelectric focusing (IEF) gel electrophoresis was performed following the method of O'Farrell [1975]. Constant voltage electrophoresis was performed at 400 V for 17 h followed by 800 V for 1 h and the gels were fixed with 15% w/v trichloroacetic acid at room temperature for 2 h, cleared with 10% methanol and 10% acetic acid, and either stained with Coomassie blue or dried for autoradiographic detection of radiolabeled actins [Strauch and Rubenstein, 1984a].

Actin Amino-Terminal Peptide Analysis

The soluble fraction of L-[^{35}S]cysteine-labeled BC3H1 myocytes was removed by treating monolayers with lysis buffer as described above. Lysed cell remnants remaining attached to the culture dishes were further extracted for 10 min on ice with smooth muscle relaxation buffer consisting of lysis buffer supplemented with 5 mM ATP and 0.1 mM EGTA. Material released by this treatment (ATP/EGTA fraction) was collected, leaving behind extraction-resistant material referred to as the cytoskeleton fraction. Total actin was isolated from all three fractions using DNase I affinity chromatography as described above. Purified, radiolabeled actin was oxidized with performic acid and digested for 2.5 h at 22°C with 10 μg/ml of tosylphenylalanylchloromethyl ketone (TPCK)-trypsin (Worthington, Freehold, NJ) in 0.1 M ammonium bicarbonate as described previously [Strauch and Rubenstein, 1984b]. Actin peptides were lyophilized to dryness and then resuspended in pyridine acetate buffer, pH 6.3 (pyridine:acetic acid:water; 25:1:225, v/v), and applied to cellulose thin layer electrophoresis plates (160 μm thick, Eastman Kodak). Constant voltage (400 V) electrophoresis was performed at pH 6.3 using the above pyridine acetate buffer and autoradiographs were prepared by exposing thoroughly dried thin layer plates to X-ray film for varying periods. Selected actin tryptic peptides were eluted from cellulose plates with water, lyophilized to dryness, dissolved in pyridine acetate buffer, pH 3.3 (pyridine:acetic acid:water; 1:25:225, v/v), subjected to a second round of electrophoresis at pH 3.3 at 400 V constant voltage, and visualized by autoradiography to unambiguously identify each actin isoform NH_2-terminal peptide [Strauch and Reeser, 1989].

RESULTS

BC3H1 myogenic cell differentiation is accompanied by extensive changes in cytoarchitectural organization. The VSM α-actin gene is activated during myoblast cytodifferentiation and its encoded product accounts for approximately half of the actin expressed by fully differentiated myocytes [Strauch and Rubenstein, 1984a; Strauch and Reeser, 1989]. To investigate the role that VSM α-actin may play in promoting cytoarchitectural changes in BC3H1 myogenic cells, we developed methods to examine how adjacent actin monomers interacted during actin thin filament assembly during myoblast differentiation. The approach employs a bifunctional protein crosslinking reagent that forms actin dimers by crosslinking polymerized actin monomers in situ. N,N′-1,4-phenylenebismaleimide (PBM) has been shown to form covalent crosslinks between adjacent actin monomers within F-actin at amino acid residues Cys 374 and Lys 191 [Knight and Offer, 1978; Elzinga and Phelan, 1984].

The properties and utility of PBM were examined in experiments that utilized purified F-actin isolated from both muscle and non-muscle sources. F-actin was reacted with PBM at a molar ratio of 0.5:1.0 (PBM:actin) for varying periods at 22°C and the resulting crosslinked actin species were evaluated by SDS-PAGE. The data shown in Figure 1 (top panel) indicate that a crosslinking time of 15 min generated a substantial amount of actin dimer. Longer periods of crosslinking (30 and 60 min) also were investigated, which produced more actin trimer and higher molecular weight oligomers but did not significantly enhance the yield of actin dimer (data not shown). Moreover, PBM was able to crosslink both muscle and non-muscle actin isoforms with approximately similar efficiency (Figure 1, middle and bottom panels). We also examined the ability of PBM to crosslink adjacent G-actin monomers contained within alternative supramolecular forms of actin such as filament bundles or non-filamentous/aggregated forms of actin that have been detected in several types of cultured cells [Cao et al, 1993]. We reasoned that this analysis could indicate the sub-cellular derivation of PBM-crosslinked species particularly if actin dimers generated from bundles or aggregates migrated differently on SDS gels compared to actin dimers from single F-actin filaments. Preparations of muscle F-actin were modified to produce both actin bundles and actin aggregates for subsequent treatment with PBM (Fig. 2). Although PBM did not crosslink G-actin monomers, F-actin filament bundles that were formed using a polymerization buffer supplemented with 50 mM $MgCl_2$ reacted with PBM and produced dimers that exhibited the same mobility as those resulting from the actin of PBM on individual F-actin filaments (Fig. 2, left panel). We referred to this crosslinked product as P-dimer to signify derivation from *polymerized* F-actin. In contrast, dimers derived from preparations of sonicated F-actin exhibited a distinctly different electrophoretic mobility on SDS gels (Fig. 2, right panel). Sonication disrupts F-actin by causing the mechanical dissociation of bound ADP from its actin monomer constituents [Gillibrand, 1972; Yanagida et al., 1974; Strzelecka-Golaszewska et al., 1975]. The crosslinked product formed by the action of PBM on a pool of *dissociated* actin filaments was referred to as D-dimer. A similarly migrating dimer was noted by previous investigators in studies of PBM crosslinked actin dimers generated during the first few seconds of G-actin polymerization [Millonig et al., 1988].

To extend these initial observations and investigate actin monomer interactions in situ, BC3H1 cells at different stages of cytodifferentiation (sub-confluent myoblasts, pre-confluent myoblasts, post-confluent myoblasts, and fully differentiated myocytes) were extracted using a cytoskeleton stabilization buffer [Fey et al., 1984] and the resulting fractions subjected to PBM crosslinking. Since PBM crosslinks only adjacent monomers contained within actin supramolecular assemblies, and not randomly associated G-actin monomers in solution (Fig. 2), this reagent permits a study of how monomers interact to form native actin structures. Actin released during extraction was referred to as the soluble fraction while lysed cell remnants remaining adhered to the tissue culture substrate represented the detergent-insoluble, actin-rich cytoskeleton fraction. Electron microscopic analysis of immunogold-labeled BC3H1 cytoskeletons following lysis in stabilization buffer revealed numerous, well-preserved actin filament bundles that were decorated along their lengths and ends with actin-specific monoclonal antibodies (data not shown). The soluble and cytoskeleton fractions were treated with PBM for 15 min at 22°C to generate actin

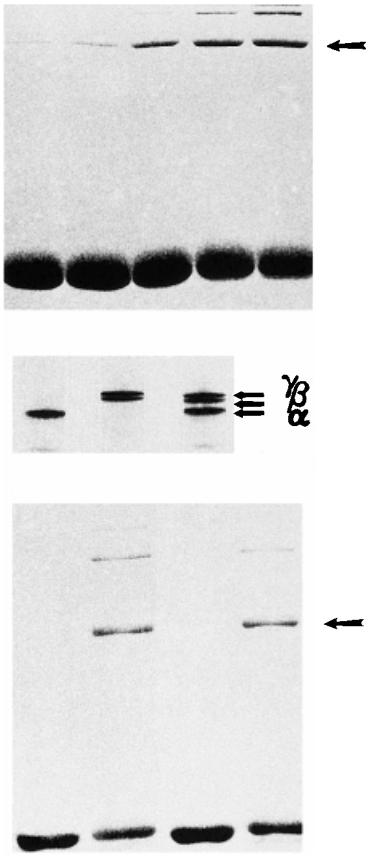

Fig. 1. Reactivity of F-actin with PBM. **Top:** SDS-PAGE depicting time-course analysis of PBM-crosslinking. Rabbit muscle F-actin was crosslinked at 22°C with PBM for 1, 2, 5, 10, and 15 min (from left to right). Actin dimer resolved on this 10% polyacrylamide gel is indicated by the arrow. **Middle** and **bottom:** Comparison of non-muscle and muscle actin crosslinking with PBM. Non-muscle G-actins (β- and γ-actin) were isolated from bovine brain, polymerized into F-actin, and crosslinked with PBM crosslinking for 15 min at 22°C. The middle panel depicts IEF gel analysis of each preparation demonstrating the distinctly different electrophoretic behavior of, from left to right, muscle actin, brain actin, and a mixture of the muscle and brain actins. The bottom panel shows a SDS gel resolving the products of PBM crosslinking. From left to right the lanes show native muscle F-actin, crosslinked muscle F-actin, native brain F-actin, and crosslinked brain F-actin. Actin dimer is indicated by an arrow.

dimers. After quenching unreacted PBM with β-mercaptoethanol, the total actin pool in each fraction (crosslinked and non-crosslinked forms) was isolated by DNase-I affinity chromatography and subjected to SDS-PAGE and immunoblot analysis using a pan-reactive actin monoclonal antibody (Mab C4). The Mab C4 immunoblot presented in Figure 3 illustrates the outcome of a typical in situ crosslinking experiments. Besides P-dimer, which was identified based on co-migration with the major crosslinked species seen in PBM-treated F-actin, a novel crosslinked actin species also appeared in both the cytoskeleton and soluble fractions at all stages of development. The mobility of this novel actin species was identical to that of D-dimer detected in crosslinked preparations of sonicated F-actin (Fig. 2). As evident in Figure 3, D-dimer was the major dimer form present in the soluble fraction from all developmental stages whereas in the actin cytoskeleton, the P-dimer form was dominant. However, fully differentiated myocytes also accumulated D-dimer in the cytoskeleton fraction (Fig. 3, group 4). Near segregation of P-dimer and D-dimer pools was most apparent in post-confluent myoblasts just before their differentiation into myocytes (Fig. 3, group 3).

Both actin dimer forms detected in crosslinked BC3H1 cell fractions reacted with two different actin-specific antibodies, bound DNase-I, and exhibited the same electrophoretic mobility as dimers present in crosslinked preparations of purified muscle actins (Figs. 2 and 3, also see Millonig et al., 1988). The mobility of D-dimer on SDS gels was faster than that theoretically expected for an actin dimer but identical to that reported for a class of PBM-crosslinked actin dimers generated during the first few seconds of monomer polymerization [Millonig et al., 1988]. We employed peptide mapping techniques to confirm that the P- and D-dimer species generated in BC3H1 cells by PBM crosslinking consisted solely of actin peptides. BC3H1 myocytes were radiolabeled with [^{35}S]cysteine, fractionated, and crosslinked, and the total actin pool was isolated using DNase-I affinity chromatography and size fractionated by SDS-PAGE. D-dimer and P-dimer bands were identified, electrophoretically eluted from gel slices, and subjected to complete digestion with TPCK-trypsin. Although the amount of radioactivity recovered in trypsin-digest products was low, laser densitometric analysis of autoradiographs revealed the same pattern of peptides in both dimer digests (Fig. 4). Taken together with the antibody and DNase-I binding properties of D-dimer, as well as previous reports showing an identical PBM-crosslinked product in studies on pure muscle actin, the peptide map data support contention that dimers in BC3H1 cells were composed of actin subunits.

From the crosslinking studies on both purified actins and fractionated BC3H1 cells, it appeared that D-dimer might be derived from a

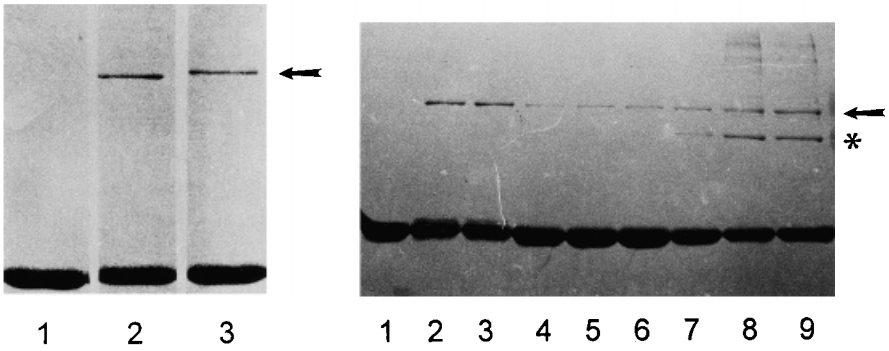

Fig. 2. Analysis of actin dimers generated by PBM crosslinking of alternative forms of actin. **Left:** G-actin monomers (**lane 1**), actin magnesium paracrystals (**lane 2**), and F-actin filaments (**lane 3**) were treated with PBM for 10 min at 22°C and then analyzed by SDS-PAGE. P-actin dimers (arrow) derived from both polymerized forms of actin (lanes 2 and 3) exhibited approximately the same mobility and abundance compared to unpolymerized G-actin (lane 1), which did not form dimers. **Right:** Non-filamentous actin aggregates were generated by sonicating muscle F-actin for 0, 1, 2, 5, 10, 30, 60, and 90 s (**lanes 2** to **9**) and then immediately treated with PBM. Sonicated, crosslinked actin preparations contained a novel actin dimer referred to as "D-dimer" (asterisk). Actin P-dimer is indicated by an arrow. Dimers were not detected in PBM-treated G-actin (**lane 1**).

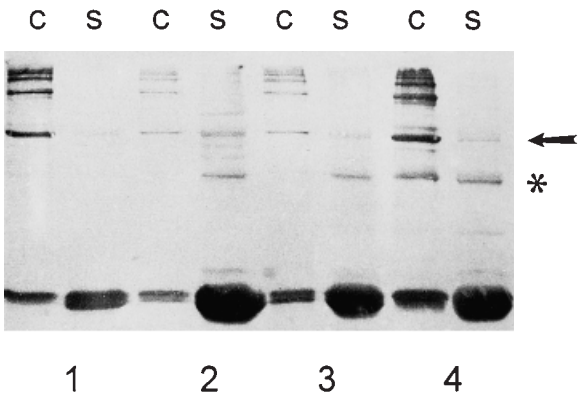

Fig. 3. Distribution of PBM-crosslinked actins in BC3H1 subcellular compartments at various developmental stages. Shown on this immunoblot are actin monomers and oligomers present in the cytoskeleton (C) and soluble (S) fractions of sub-confluent myoblasts (group 1), pre-confluent myoblasts (group 2), transitional-stage, post-confluent myoblasts (group 3), and fully differentiated myocytes (group 4). Actin P-dimer and D-dimer are labeled on the right with an arrow and asterisk, respectively. The C4 monoclonal antibody is a pan-specific antibody that binds all actin isoforms.

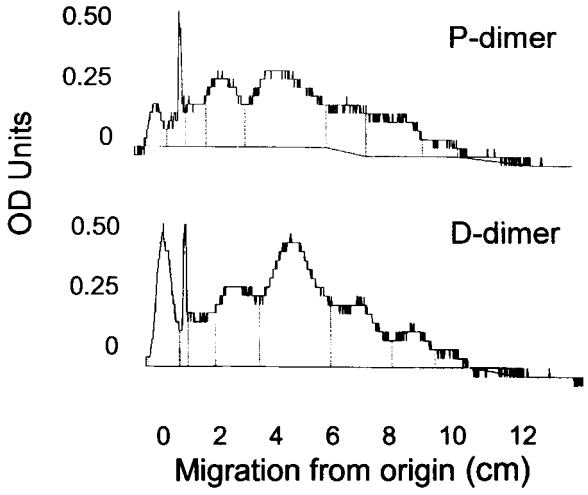

Fig. 4. Densitometric analysis of tryptic peptides derived from affinity-purified actin P-dimer and D-dimer. Post-confluent BC3H1 myoblasts were radiolabeled with L-[^{35}S]cysteine, fractionated, and crosslinked as described in Methods. Actin was isolated from the combined cytoskeleton and soluble fractions using DNase-I affinity chromatography. P-dimer and D-dimer species were resolved by SDS-PAGE, eluted from gel slices, and digested with TPCK-trypsin. Tryptic peptides were resolved by cellulose thin layer electrophoresis in pyridine acetate, pH 6.3, and evaluated by autoradiography and laser densitometry. The origin of electrophoresis is indicated by 0 on the x-axis.

pool of non-filamentous actin whereas P-dimer was most likely produced by the reaction of PBM with F-actin stress fibers within the cytoskeleton. We examined if there was a dynamic relationship between these two actin compartments by following the distribution of pulse-labeled actin monomer between P-dimer and D-dimer pools. To determine the optimum conditions for effective pulse labeling, BC3H1 myoblasts and myocytes were radiolabeled with varying amounts of L-[^{35}S]methionine for different time periods and then analyzed for incorporation into actin by SDS-PAGE and autoradiography. A labeling period of 10 min using 50 µCi/ml of L-[^{35}S]methionine provided for adequate signal detection without saturation of the intracellular methionine pool. Previous studies also indicated that BC3H1 cells that were pulse labeled for periods up to 20 min can still be efficiently chased [Strauch and Ruben-

stein, 1984b]. Post-confluent myoblasts were pulse labeled, washed thoroughly with PBS, and placed into chase medium containing excess unlabeled methionine and cysteine. At the end of each chase period, the cells were fractionated and crosslinked with PBM as described previously. Crosslinked actin species were isolated using DNase-I chromatography and the entire bound fraction from each sample was analyzed by SDS-PAGE. As shown in Figure 5, D-dimer was restricted to the cytoskeleton after the 10-min pulse but appeared in the soluble fraction during the chase and ultimately was confined to the soluble fraction after 1 h. In contrast, P-dimer was detected only in the cytoskeleton fraction during both the pulse and chase. The results imply that actin monomers organized as D-dimer are more dynamic than monomers contained in F-actin in the sense that they appear to transit sequentially through the filamentous and non-filamentous actin compartments in maturing, post-confluent BC3H1 myoblasts. The initial association of newly formed D-dimer with the cytoskeleton may be obligatory in view of possible physical links between the actin mRNA translational machinery and the cytoskeleton [Fulton et al., 1980].

Dynamic aspects of D-dimer and P-dimer compartmentalization also were investigated using fully differentiated myocytes and myocytes treated with EDTA (EDTA-myocytes). Since myocytes are post-mitotic and maintained in serum-free medium, the size and stability of actin dimer pools in these cells reflect aspects of actin utilization that are independent of cell proliferation. EDTA promotes rapid, synchronous cytoskeletal re-arrangements in myocytes due to the disruption of cell-cell and cell-matrix contacts necessary to maintain the differentiated cell phenotype [Strauch et al., 1992]. EDTA causes highly elongated myocytes to assume a broad, fibroblastoid shape although the cells do not proliferate since they are retained in serum-free medium. The EDTA-myocyte model therefore permitted study of actin dimer dynamics during remodeling of pre-existing cytoskeletal elements. Myocytes were pulse labeled for 10 min using 50 μCi/ml of L[^{35}S]methionine and treated with 0.1% EDTA in PBS for 5 min at 37°C. The released myocytes were dispersed by gentle pipetting and re-seeded into fresh culture dishes using serum-free N2 medium. Since a recovery period of 2 h was required for complete reattachment, the chase period was extended to 5 h, after which time the myocytes were fractionated and crosslinked with PBM. Crosslinked actin species were isolated using DNase-I affinity chromatography and analyzed by SDS-PAGE. Fully differentiated myocytes apparently retained D-dimer in the cytoskeleton during the chase period, implying that this actin was stably associated with actin filaments in developmentally advanced BC3H1 cells (Fig. 6). This was in constrast to results obtained in the pulse-chase analysis of D-dimer in immature myoblasts (Fig. 5). However, when myocytes assumed an immature, myoblast-like appearance following treatment with EDTA, D-dimer became depleted from the cytoskeleton during the chase (Fig. 6). These results implied that experimentally induced cytoskeletal rearrangements were accompanied by changes in the distribution of actin monomers involved in the formation of D-dimers. Thus, segregation of P- and D-dimers between cytoskeleton and soluble fractions was most pronounced in both rapidly maturing, post-confluent myoblasts (Fig. 5) and de-differentiated, sub-confluent EDTA-myocytes (Fig. 6), which represent the two preparations of BC3H1 cells that are most actively engaged in actin cytoarchitectural remodeling.

The co-existence of multiple forms of actin in smooth muscle cells implies that there may be a physiological requirement for different types of actin filaments in the vasculature or gut. Some investigators have proposed that there are two populations of microfilaments in smooth muscle

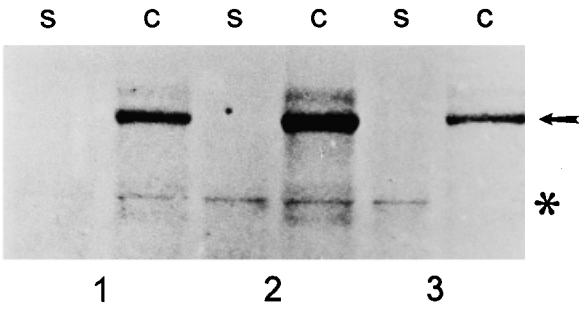

Fig. 5. Dynamic relationship between the actin D-dimer and P-dimer pools in developing BC3H1 myoblasts. Post-confluent BC3H1 myoblasts were radiolabeled with L-[^{35}S]methionine for 10 min, chased for 0 (group 1), 30 (group 2), and 60 (group 3) min, and fractionated into soluble (S) and cytoskeleton (C) compartments. Each fraction first was treated with PBM and then crosslinked actins were purified using DNase-I affinity chromatography and analyzed by SDS-PAGE and autoradiography. Actin P-dimer and D-dimer are noted by an arrow and asterisk, respectively.

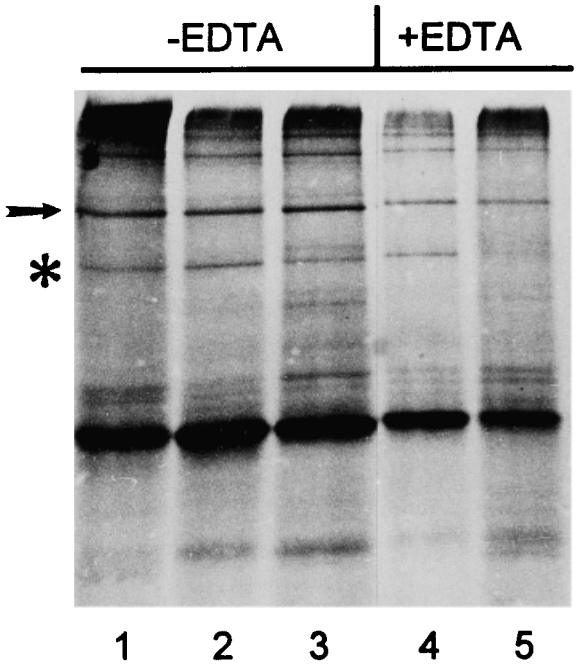

Fig. 6. Pulse-chase analysis of actin dimers in the cytoskeleton fraction of differentiated BC3H1 myocytes following dispersion of cell-matrix contacts with EDTA. EDTA treatment modulates myocyte morphology without promoting cell proliferation. Shown are crosslinked actin samples isolated by DNase-I affinitychromatography from the cytoskeleton fractions of L-[^{35}S]methionine pulse-labeled myocytes (50 μCi/ml, 10-min pulse, lane 1) or from pulse-labeled myocytes that subsequently were chased for 1 h (lanes 2,4) or 3 h (lanes 3,5) either with (lanes 4,5) or without (lanes 2,3) EDTA dispersion. Myocytes were chased in N2 serum-free medium (refer to Methods). Actin P-dimer is noted by the arrow and D-dimer is indicated with an asterisk.

tissues: a contractile group associated with caldesmon and/or myosin, and a cytoskeleton group that is linked to dense body proteins such as desmin or filamin [Furst et al., 1986; Lehman et al., 1987; Small et al., 1986]. In contrast, other investigators reported that the distribution of vascular smooth muscle α-actin and the nonmuscle actins was no different in arterial smooth muscle thin filaments obtained from cell and tissue extracts [Drew et al., 1991]. We addressed this unresolved question by investigating the in situ distribution of VSM α-actin in cellular fractions prepared from BC3H1 myogenic cells. Having determined that P-dimer represented crosslinked actin monomers from F-actin filaments and D-dimer was derived from crosslinked monomers found in non-filamentous actin structures, we employed a VSM α-actin-specific antibody to examine the isoform composition and distribution of crosslinked actin species during BC3H1 myoblast differentiation. This approach allowed us to examine how newly synthesized VSM α-actin monomers become integrated into filamentous and non-filamentous actin elements within developing myocytes. As shown in Figure 7, expression of VSM α-actin polypeptide was highest in fully differentiated myocytes [Strauch and Reeser, 1989]. VSM α-actin was first detected in post-confluent myoblasts but only in the cytoskeleton fraction as P-dimer. Surprisingly, however, VSM α-actin protein was observed only in higher molecular weight multimers in these transitional-stage myoblast cytoskeletons; very little uncrosslinked monomeric VSM α-actin was detected in these preparations (Fig. 7). The data suggested that newly synthesized VSM α-actin polypeptides were very rapidly assembled into F-actin filaments in the developing myoblast cytoskeleton and nearly all monomer subunits had been crosslinked by PBM to form P-dimer and larger multimers. When VSM α-actin expression reached a steady-state level in myocytes, abundant monomeric actin was detected by Mab 1A4. D-dimer was evident in both fractions from fully differentiated myocytes but it appeared to be the sole form of dimer detected in the soluble fraction of these cells.

The results shown in Figure 7 implied that VSM α-actin might be specifically segregated in the cytoskeleton during myoblast differentiation. We prepared tryptic peptide maps to determine if actin isoform domains were present in myocytes. BC3H1 myocytes were lysed in situ to generate the soluble and cytoskeleton fractions as described above. Subsequent to cell lysis, a smooth muscle relaxation buffer consisting of lysis buffer supplemented with 5 mM ATP and 0.1 mM EGTA was applied to the myocyte cytoskeleton to further extract actin that may be complexed with myosin [Sobieszek and Small, 1977]. The material released by this treatment was referred to as the ATP/EGTA fraction and the remaining residue on the culture dish was termed the cytoskeleton fraction. Total actin was isolated from each fraction using DNase-I affinity chromatography and subjected to tryptic peptide map analysis to identify the various actin isoforms in each fraction. As shown in Figure 8, both non-muscle and VSM α-actin were released during initial lysis of myocytes. However, subsequent treatment with ATP/EGTA released only non-muscle actins (β- and γ-actin), leaving a VSM α-actin enriched cytoskeleton on the culture dish. Sec-

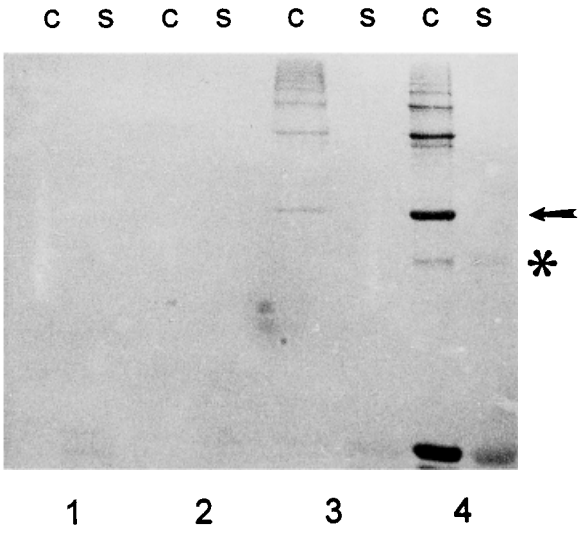

Fig. 7. Distribution of PBM-crosslinked VSM α-actin in developing BC3H1 cells. The 1A4 antibody used in this immunoblot analysis binds only to the VSM α-actin isoform. Undifferentiated, sub-confluent (group 1) and pre-confluent (group 2) myoblasts contain only non-muscle actins and do not react substantially with the 1A4 antibody. VSM α-actin accumulated in transitional stage, post-confluent myoblasts (group 3), but only in the cytoskeleton (C), as P-dimer (arrow) and high molecular weight crosslinked species. In fully differentiated myocytes (group 4), VSM α-actin appeared predominantly in the cytoskeleton with a small amount noted in the soluble fraction (S). The asterisk denotes VSM α-actin D-dimer that was observed only in myocytes (group 4).

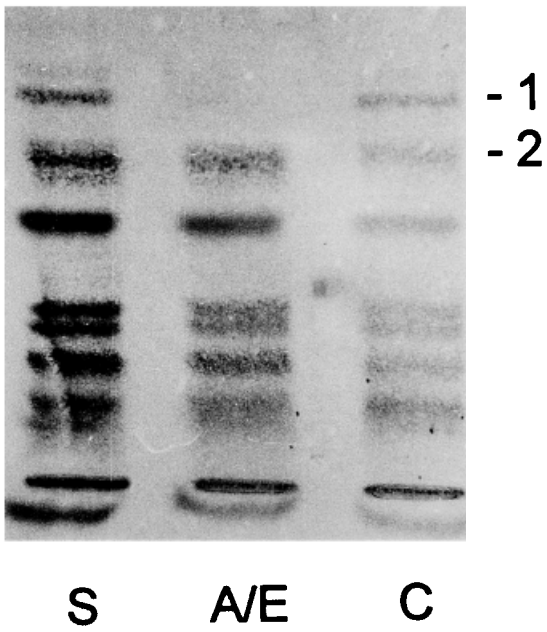

Fig. 8. Selective actin isoform compartmentalization in BC3H1 myocytes. Fully differentiated myocytes expressing non-muscle β- and γ-actins and VSM α-actin were labeled with L-[^{35}S]cysteine. Actins were isolated from each of three sub-cellular fractions by DNase-I affinity chromatography and analyzed using tryptic peptide mapping techniques. Actin was isolated from cytoplasmic proteins released from myocytes following the initial lysis (S), the fraction released following treatment with 5 mM ATP and 0.1 mM EGTA (A/E), and the extraction-resistent cytoskeleton remnant (C). Individual actin N-terminal tryptic peptides were resolved by pH 6.3 thin layer electrophoresis and autoradiography. ATP/EGTA selectively dissociates non-muscle actins (peptide 2) whereas the cytoskeleton appears to be enriched for the VSM α-actin isoform (peptide 1).

ondary thin layer electrophoresis at pH 3.3 confirmed the identity of each actin N-terminal tryptic peptide resolved on pH 6.3 electrophoretograms (data not shown). Moreover, at least a portion of the PBM-crosslinked, non-muscle actin released by ATP/EGTA extraction was in filamentous form since P-dimer was the major dimer species detected when the released actin was analyzed by SDS-PAGE (Figure 9, left panel). D-dimer was the dominant dimer in the soluble fraction whereas the cytoskeleton residue, much like the ATP/EGTA fraction, contained more P-dimer. Immunoblot analysis of these samples using the VSM α-actin-selective 1A4 monoclonal antibody confirmed that the cytoskeleton was highly enriched for VSM α-actin whereas both the initial lysis and subsequent ATP/EGTA extraction removed primarily non-muscle β- and γ-actins that did not react with the 1A4 antibody (Fig. 9, right panel). Isoelectric focusing electrophoresis revealed only non-muscle β- and γ-actins in the ATP/EGTA fraction, which confirmed the negative reaction of this material with the α-actin-specific 1A4 antibody (Fig. 9, bottom panel). Results presented in Figure 9 are consistent with the suggestion that BC3H1 myocytes contain a pool of non-muscle actin-enriched F-actin filaments that differ from VSM α-actin filaments with respect to their spatial compartmentalization and/or resistance to biochemical extraction.

DISCUSSION

Two distinct actin dimer species (P-dimer and D-dimer) were detected when a bifunctional protein crosslinker was used to covalently link actin monomers in BC3H1 myogenic cells. Several lines of evidence support the idea that P-dimer was generated from F-actin. Most significantly, P-dimer was consistently observed to be the dominant dimer species in cytoskeletons that contained numerous F-actin filament bundles. The extraction conditions we employed specifically stabilized F-actin fila-

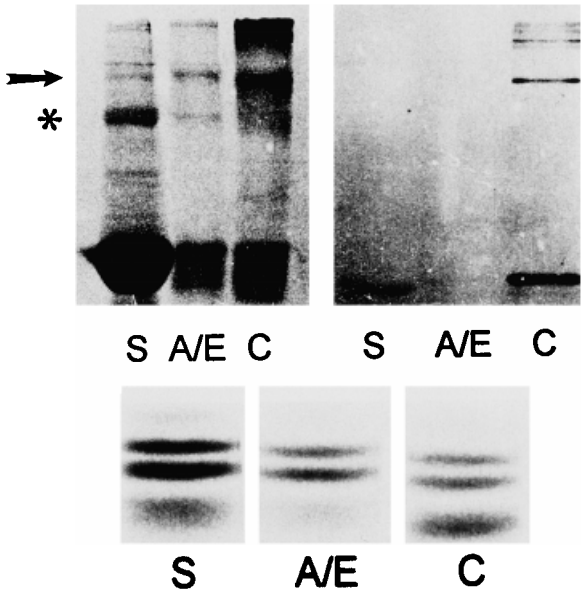

Fig. 9. Supramolecular organization of non-muscle and smooth muscle actins in BC3H1 myocytes. Fully differentiated myocytes were lysed and both the released, soluble actin (S) and actin remaining associated with the lysed myocyte remnants were crosslinked with PBM. Subsequently, the crosslinked remnants were further extracted with 5 mM ATP and 0.1 mM EGTA. The released, crosslinked actins were collected (A/E), leaving behind actins that were stably associated with the extraction-resistent cytoskeleton (C). Actins were purified from each fraction using DNase-I affinity chromatography and analyzed by SDS-PAGE (**left**) immunoblot using the smooth muscle actin-selective 1A4 antibody (**right**) or isoelectric focusing electrophoresis (**bottom**). P-dimer and D-dimer are indicated by an arrow and asterisk, respectively. In the bottom panel, the upper and lower bands in the ATP/EGTA fraction correspond to non-muscle γ- and β-actin, respectively.

ments, as confirmed by both biochemical and microscopic analyses. P-dimer abundance thus reflected the presence of F-actin in cells at the time of lysis and crosslinking. In contrast, D-dimer was more abundant than P-dimer in the soluble fraction of lysed BC3H1 cells. D-dimer also was demonstrated to represent actin homodimer based on its affinity for DNase-I, reactivity with actin-specific antibodies, and tryptic peptide map similarity to both P-dimer and monomeric G-actin. Moreover, D-dimer was formed when pure preparations of sonicated F-actin were crosslinked with PBM. Other investigators also have observed D-dimer products when purified muscle actin was treated with PBM at the very start of monomer polymerization [Millonig et al., 1988]. Taken together, these observations implied that D-dimer was derived from a non-filamentous actin supramolecular entity in BC3H1 muscle cells. Our report is the first to identify multiple arrangements of actin monomers in muscle cells. Actin monomers may be paired in different ways to facilitate the formation of alternative supramolecular assemblies during muscle cell development.

Other investigators have reported that two actin dimer species were obtained when purified muscle F-actin was reacted with PBM. Millonig et al. described a "lower" dimer (LD), which exhibited the same electrophoretic mobility as D-dimer when PBM was added to actin solutions within the first 30 s of polymerization [Millonig et al., 1988]. Further analysis suggested that actin dimerization and LD formation was the first step of the actin polymerization process. During polymerization, a second type of actin dimer, "upper" dimer (UD), accumulated, which appears to be identical to P-dimer detected in our studies of crosslinked BC3H1 cell cytoskeletons. UD was shown to arise when PBM crosslinks Cys-374 and Lys-191 on adjacent actin monomers in the F-actin filament [Elzinga and Phelan, 1984]. LD mostly likely is formed when PBM links Cys-374 and Cys-374 in anti-parallel monomers residing within non-filamentous actin structures [Millonig et al., 1988]. In native F-actin, Cys-374 residues in adjacent monomers are not close enough to be crosslinked by PBM [Kabsch and Vandekerckhove, 1992]. Our identification of D-dimer in native muscle cells indicates that some actin monomers apparently are assembled into anti-parallel arrays, which involve carboxy termini interactions across the short distance (1.2 nm) required for efficient PBM crosslinking. D-dimer formation could be facilitated by actin monomer conformational changes [Millonig et al., 1988] or by association with other cellular factors. Recently, Bubb et al. reported that Swinholide A-actin dimer complexes exhibited the same electrophoretic mobility as D-dimer when subjected to crosslinking in low ionic strength buffer containing PBM [Bubb et al., 1995]. In addition, the actin dimers that were formed as a result of the severing action of gelsolin on F-actin filaments resembled D-dimer rather than P-dimer [Hesterkamp et al., 1993]. Further studies of the D-dimer species may not only help to clarify the molecular organization of non-filamentous actin in developing muscle cells but also indicate if anti-parallel D-dimer complexes can nucleate F-actin filament assembly during myofibrillogenesis. In

this regard, D-dimers began to accumulate in the soluble fraction as myoblasts matured into myocytes. These early D-dimers were composed of non-muscle actin since they did not react with the smooth muscle actin-specific 1A4 antibody. However, their formation appears to occur concurrently with myoblast differentiation. One possible explanation is that the pre-existing non-muscle actin cytoskeleton becomes remodeled to accommodate large smooth muscle α-actin stress fiber bundles that occupy virtually all available space in highly elongated myocytes. A transient increase in the D-dimer level may facilitate cytoskeletal remodeling and actin stress fiber formation in maturing myoblasts because this type of dimer has been proposed to nucleate F-actin filament assembly [Millonig et al., 1988].

Mechanisms that control the size of the intracellular pool of unpolymerized actin are potentially important in controlling both the rate and extent of actin polymerization. When Cao and colleagues visualized actin pools in non-muscle cells using labeling agents that differed with respect to their affinity for filamentous or non-filamentous forms of actin, they found that non-filamentous actin was distributed primarily at the cell periphery in the form of punctuate structures [Cao et al., 1993]. Although the functional significance of non-filamentous actin foci is not well understood, some evidence suggests that they might represent sites of nascent F-actin polymerization [Spudich et al., 1988; Bonder et al., 1989]. We also observed similar non-filamentous actin domains in the BC3H1 myocyte cytoskeleton. Using an immunogold detection technique to probe actin distribution, it was evident that the VSM α-actin-specific 1A4 antibody bound actin clusters located primarily at the ends of actin filament bundles [Qu et al., unpublished observations]. We do not know if these actin clusters are the morphological equivalent of D-dimers or non-filamentous actin described by other investigators [Cao et al., 1993]. The rapid depletion of D-dimer from the cytoskeleton observed in pulse-chase experiments using EDTA-remodeled myocytes suggested that D-dimer may be rapidly utilized to assemble actin filament or bundle systems in these cells. The proximity of actin clusters to filament ends noted in electron microscopic studies of the myocyte cytoskeleton would be consistent with this suggestion and warrants further investigation.

Co-expression of VSM α-actin and non-muscle actins in differentiated BC3H1 myocytes make this cell line a useful model to examine questions about selective actin isoform utilization. Having developed a crosslinking approach to study actin monomer interaction in situ, we examined the distribution of VSM α-actin in BC3H1 cells using an actin isoform-specific antibody. As expected, we found that VSM α-actin first appeared in post-confluent myoblasts but what was most striking was the enrichment of this isoform in actin polymers (P-dimer, trimer, tetramer, and larger oligomers). This observation strongly suggested that, at the early stages of BC3H1 cell differentiation, virtually all newly synthesized VSM α-actin was selectively polymerized into the F-actin-enriched cytoskeleton. We further addressed the question of actin compartmentalization by looking at the native distribution of isoforms following biochemical extraction. We applied a smooth muscle relaxation buffer to the lysed myocytes to specifically release actin filaments from myosin complexes. Non-muscle actins were preferentially released by this treatment, further supporting the notion that VSM α-actin was compartmentalized differently from the more easily released non-muscle actins. Interestingly, a substantial amount of non-muscle actin also remained associated with the detergent-insoluble cytoskeleton, implying that not all of this actin isoform could be dissociated with relaxation buffer. This observation was consistent with morphological data presented by North et al. showing the localization of non-muscle actin in dense body-associated compartments in avian gizzard smooth muscle cells [North et al., 1994]. Our data do not address the question of whether intrinsic resistence of the cytoskeleton to biochemical extraction was due to the portion of the non-muscle actin pool that remained associated with lysed myocyte remnants following extraction or because of the relatively high degree of enrichment for VSM α-actin F-actin in the cytoskeleton. In this regard, actin isoform homopolymers may have unique biochemical properties that could contribute to differential extractability noted in our studies on BC3H1 myocytes. At least some filament systems in BC3H1 cells may be homogenous with respect to actin isoform composition since the non-muscle actin extracted from myocytes with ATP and EGTA apparently was in the F-actin form

because it yielded P-dimer when treated with PBM.

The efficient polymerization of VSM α-actin noted during the early stages of myoblast differentiation implied that mechanisms exist in BC3H1 myogenic cells that govern the selective targeting of VSM α-actin mRNA and/or newly synthesized polypeptides to sub-cellular sites of F-actin assembly. We do not know if enrichment of VSM α-actin in the cytoskeleton was due to differences in translational efficiency between mRNAs associated with free polysomes vs. those anchored to the cytoskeleton or because VSM α-actin polypeptide is targeted preferentially to the growing filament ends of the stress fiber-enriched cytoskeleton. Although the N-terminal regions of actin isoform polypeptide chains carry different charge to mass ratios and are capable of interacting with a variety of actin-binding proteins, future efforts to elucidate the molecular mechanisms of selective actin isoform utilization must also consider important differences in C-terminal polypeptide regions as well. As demonstrated by von Arx and coworkers in studies on transfected cardiomyocytes, chimeric actin molecules were observed to partition according to the composition of the C-terminal region encompassing residues 84–374 [von Arx et al., 1995]. While chimeric actins containing cardiac α-actin-specific amino acids in this segment of the polypeptide chain were distributed normally in sarcomeres, actins harboring non-muscle γ-actin-specific residues at the C-terminus were distributed at the cell periphery and excluded from the sarcomere-rich, central perinuclear area. Compartmentalization of actin isoforms also could be governed at the mRNA level. Hill and Gunning showed that non-muscle γ-actin mRNA was distributed differently from non-muscle β-actin mRNA in myoblasts, with γ-actin mRNA displaying only perinuclear localization while β-actin mRNA resided in both perinuclear and peripheral locations [Hill and Gunning, 1993]. Determinants of actin mRNA localization have been linked to elements contained within isoform specific 3′-untranslated sequences [Kislauskis et al., 1993, 1994]. This observation suggests that inherent differences in actin mRNA structure may govern sorting of actins into separate cytoarchitectural components. However, this does not appear to be the basis for enrichment of VSM α-actin mRNA in the myocyte cytoskeleton since analysis of VSM α-actin mRNA distribution in transfected cells using β-galactosidase target mRNA linked to the VSM α-actin 3′UT region did not reveal selective association with the cytoskeleton [Qu et al., unpublished observations]. Thus, our findings best support the idea that compartmentalization is based on some intrinsic feature of the VSM α-actin polypeptide that cause it to become highly localized in muscle cell actin filament bundles.

REFERENCES

Black FM, Packer SE, Parker TG, Michael LH, Roberts R, Schwartz RJ, Schneider MD (1991): The vascular smooth muscle α-actin gene is reactivated during cardiac hypertrophy provoked by load. J Clin Invest 88:1581–1588.

Bonder EM, Fishkind DJ, Cotran NM, Begg DA (1989): The cortical actin-membrane cytoskeleton of unfertilized sea urchin eggs: Analysis of the spatial organization and relationship of filamentous actin, nonfilamentous actin, and egg spectrin. Dev Biol 134:327–341.

Bottenstein JE, Sato GH (1979): Growth of a rat neuroblastoma cell line in serum-free supplemented medium. Proc Natl Acad Sci USA 76:514–517.

Bubb MR, Spector I, Bershadsky AD, Korn ED (1995): Swinholide A is a microfilament disrupting marine toxin that stabilizes actin dimers and severs actin filaments. J Biol Chem 270:3463–3466.

Cao L, Fishkind DJ, Wang Y (1993): Localization and dynamics of nonfilamentous actin in cultured cells. J Cell Biol 123:173–181.

Darby I, Skalli O, Gabbiani G (1990): α-Smooth muscle actin is transiently expressed by myofibroblasts during experimental wound healing. Lab Invest 63:21–29.

DeNofrio D, Hoock TC, Herman IM (1989): Functional sorting of actin isoforms in microvascular pericytes. J Cell Biol 109:191–202.

Drew JS, Moos C, Murphy RA (1991): Localization of isoactins in isolated smooth muscle thin filaments by double gold immunolabeling. Am J Physiol Cell Physiol 260: C1332–C1340.

Elzinga M, Phelan JJ (1984): F-actin is intermolecular crosslinked by N,N′-phenylenedimaleimide through Lys 191 and Cys 374. Proc Natl Acad Sci USA 81:6599–6602.

Fey EG, Capco DD, Krochmalnic G, Penman S (1984): Epithelial structure revealed by chemical dissection and unembedded electron microscopy. J Cell Biol 99:203s–208s.

Fulton AB, Wan KM, Penman S (1980): The spatial distribution of polyribosomes in 3T3 cells and the associated assembly of proteins into the skeletal framework. Cell 20:849–857.

Furst D, Cross RA, De Mey J, Small JV (1986): Caldesmon is an elongated, flexible molecule localized in the actomyosin domains of smooth muscle. EMBO J 5:251–257.

Gillibrand IM (1972): A study of aggregation phenomena occurring in actin solution during polymerization. Biochem J 127:737–739.

Herman IM (1993): Actin isoforms. Curr Opin Cell Biol 5:48–55.

Hesterkamp T, Weeds AG, Mannherz HG (1993): The actin monomers in the ternary gelsolin:2 actin complex are in an antiparallel orientation. Eur J Biochem 218:507–513.

Hill MA, Gunning P (1993): Beta and gamma actin mRNAs are differentially located within myoblasts. J Cell Biol 122:825–832.

Kabsch W, Vandekerckhove J (1992): Structure and function of actin. Annu Rev Biophys Biophys Chem 21:49–76.

Kedes LH, Stockdale FE (1989): "Cellular and Molecular Biology of Muscle Development." New York: R. Liss, Inc.

Kislauskis EH, Li Z, Singer RH, Taneja KL (1993): Isoform-specific 3′-untranslated sequences sort α-cardiac and β-cytoplasmic actin messenger RNAs to different cytoplasmic compartments. J Cell Biol 123:165–172.

Kislauskis EH, Zhu X, Singer RH (1994): Sequences responsible for intracellular localization of β-actin messenger RNA also affect cell phenotype. J Cell Biol 127:441–451.

Knight P, Offer G (1978): p-NN′-phenylenebismaleimide, a specific cross-linking agent for F-actin. Biochem J 175: 1023–1032.

Kocher O, Gabbiani G (1987): Analysis of α-smooth-muscle actin mRNA expression in rat aortic smooth-muscle cells using a specific cDNA probe. Differentiation 34:201–209.

Korn ED (1978): Biochemistry of actomyosin-dependent cell motility (a review). Proc Natl Acad Sci USA 75:588–599.

Lazarides E, Lindberg U (1974): Actin is the naturally occurring inhibitor of deoxyribonuclease I. Proc Natl Acad Sci USA 71:4742–4746.

Lehman W, Sheldon A, Madonia W (1987): Diversity in smooth muscle thin filament composition. Biochim Biophys Acta 914:35–39.

McHugh KM, Crawford K, Lessard JL (1991): A comprehensive analysis of developmental and tissue-specific expression of the isoactin multigene family in the rat. Dev Biol 148:442–458.

Millonig R, Salvo H, Aebi U (1988): Probing actin polymerization by intermolecular cross-linking. J Cell Biol 106: 785–796.

North AJ, Gimona M, Lando Z, Small JV (1994): Actin isoform compartments in chicken gizzard smooth muscle cells. J Cell Sci 107:445–455.

O'Farrell PH (1975): High resolution two-dimensional electrophoresis of proteins. J Biol Chem 250:4007–4021.

Pardo JV, Pittenger MF, Craig SW (1983): Subcellular sorting of isoactins: Selective association of gamma actin with skeletal muscle mitochondria. Cell 32:1093–1103.

Parker TG, Schneider MD (1991): Growth factors, proto-oncogenes, and plasticity of the cardiac phenotype. Annu Rev Physiol 53:179–200.

Perriard, J-C, von Arx P, Bantle S, Eppenberger HM, Eppenberger-Eberhardt M, Messerli M, Soldati T (1992): Molecular analysis of protein sorting during biogenesis of muscle cytoarchitecture. Symp. Soc. Exp Biol 46:219–235.

Ronnov-Jessen L, Petersen OW (1996): A function for filamentous α-smooth muscle actin: Retardation of motility in fibroblasts. J Cell Biol 134:67–80.

Ruzicka DL, Schwartz RJ (1988): Sequential activation of α-actin genes during avian cardiogenesis: Vascular smooth muscle α-actin gene transcripts mark onset of cardiomyocyte differentiation. J Cell Biol 107:2575–2586.

Sappino AP, Schürch W, Gabbiani G (1990): Differentiation repertoire of fibroblastic cells: Expression of cytoskeletal proteins as marker of phenotypic modulations. Lab Invest 63:144–161.

Sawtell NM, Lessard JL (1989): Cellular distribution of smooth muscle actins during mammalian embryogenesis: Expression of the α-vascular but not the gamma-enteric isoform in differentiating striated myocytes. J Cell Biol 109:2929–2937.

Schevzov G, Lloyd C, Gunning P (1992): High level expression of transfected β- and gamma-actin genes differentially impacts on myoblast cytoarchitecture. J Cell Biol 117:775–785.

Schubert D, Harris AJ, Devine CE, Heinemann S (1974): Characterization of a unique muscle cell line. J Cell Biol 61:398–413.

Schwartz SM, Reidy MA (1987): Common mechanisms of proliferation of smooth muscle in atherosclerosis and hypertension. Hum Pathol 18:240–247.

Skalli O, Gabbiani G (1988): The biology of the myofibroblast. Relation to wound contraction and fibrocontractive diseases. In Clark RAF, Henson PM (eds): "The Molecular and Cellular Biology of Wound Repair." New York: Plenum Publishing Corp. pp 373–401.

Small JV, Furst DO, De Mey J (1986): Localization of filamin in smooth muscle. J Cell Biol 102:210–220.

Sobieszek A, Small JV (1977): Regulation of the actin myosin interaction in vertebrate smooth muscle: Activation via a myosin light-chain kinase and the effect of tropomyosin. J Mol Biol 112:559–576.

Spudich A, Wrenn JT, Wessels NK (1988): Infertilized sea urchin eggs contain a discrete cortical shell of actin that is subdivided into two organizational states. Cell Motil Cytoskeleton 9:85–96.

Spudich JA, Watt S (1971): The regulation of rabbit skeletal muscle contraction. J Biol Chem 246:4866–4871.

Strauch AR, Reeser JC (1989): Sequential expression of smooth muscle and sarcomeric α-actin isoforms during BC3H1 cell differentiation. J Biol Chem 264:8345–8355.

Strauch AR, Rubenstein PA (1984a): Induction of vascular smooth muscle α-isoactin expression in BC3H1 cells. J Biol Chem 259:3152–3159.

Strauch AR, Rubenstein PA (1984b): A vascular smooth muscle α-isoactin biosynthetic intermediate in BC3H1 cells. Identification of acetylcysteine at the amino terminus. J Biol Chem 259:7224–7229.

Strauch AR, Berman MD, Miller HR (1991): Substrate-associated macromolecules promote cytodifferentiation of BC3H1 myogenic cells. J Cell Physiol 146:337–348.

Strauch AR, Min B, Reeser JC, Yan H, Foster DN, Berman MD (1992): Density-dependent modulation of vascular smooth muscle α-actin biosynthetic processing in differentiated BC3H1 myocytes. J Cell Biochem 50:266–278.

Strzelecka-Golaszewska H, Venyamino SY, Zmozynski S, Toulmé J-J, Helene C (1975): Changes in the state of actin during superprecipitation of actomyosin. Eur J Biochem 55:221–230.

Uyemura DG, Brown SS, Spudich JA (1978): Biochemical and structural characterization of actin from *Dictyostelium discoideum*. J Biol Chem 253:9088–9096.

Vandekerckhove J, Weber K (1981): Actin typing on total cellular extracts. Eur J Biochem 113:595–603.

von Arx P, Bantle S, Soldati T, Perriard J-C (1995): Dominant negative effect of cytoplasmic actin isoproteins on cardiomyocyte cytoarchitecture and function. J Cell Biol 131:1759–1773.

Yanagida T, Taniguchi M, Oosawa F (1974): Conformational changes of F-actin in the thin filments of muscle induced in vivo and in vitro by calcium ions. J Mol Biol 90:509–522.